Jet-Inflated Cocoons in Dying Stars: New LIGO-Detectable Gravitational Wave Sources

Ore Gottlieb,[1*] Hiroki Nagakura,[2] Alexander Tchekhovskoy,[1]
Priyamvada Natarajan,[3,4,5] Enrico Ramirez-Ruiz,[6]
Jonatan Jacquemin-Ide,[1] Nick Kaaz,[1] Vicky Kalogera[1]

[1]Center for Interdisciplinary Exploration & Research in Astrophysics (CIERA), Northwestern University, 1800 Sherman Ave, Evanston, IL 60201, USA
[2]Division of Science, National Astronomical Observatory of Japan, 2-21-1 Osawa, Mitaka, Tokyo 181-8588, Japan
[3]Department of Astronomy, Yale University, 52 Hillhouse Avenue, New Haven, CT 06520, USA
[4]Department of Physics, Yale University, P.O. Box 208121, New Haven, CT 06520, USA
[5]Black Hole Initiative, Harvard University, 20 Garden Street, Cambridge MA 02138, USA
[6]Department of Astronomy and Astrophysics, University of California, Santa Cruz, CA 95064, USA
[*]Corresponding author. Email: ore@northwestern.edu.

Abstract

Long Gamma-Ray Bursts (LGRBs), the most powerful events in the Universe, are generated by jets that emerge from dying massive stars. Highly beamed geometry and immense energy make jets promising gravitational wave (GW) sources. However, their sub-Hertz GW emission is outside of ground based GW detector (LIGO) frequency band. Using a 3D general-relativistic magnetohydrodynamic simulation of a dying star, we show that jets inflate a turbulent, energetic bubble-cocoon that emits strong quasi-spherical GW emission within the LIGO band, $0.1-0.6$ kHz, over the characteristic jet activity timescale, $\approx 10-100$ s. This is the first non-inspiral GW source detectable by LIGO out to hundreds of Mpc, with $\approx 0.1-10$ detectable events expected during LIGO observing run O4. These GWs are likely accompanied by detectable energetic core-collapse supernova and cocoon electromagnetic emission, making jetted stellar explosions promising multi-messenger sources.

Intro: MM emission from ccSN

Core-collapse supernovae (CCSNe) provide a unique opportunity to study the last stages of stellar life-cycles, the synthesis of heavy elements, and the birth of compact objects (*1–3*). However, the intervening opaque stellar gas limits the prospects for learning about the underlying physics of the explosion mechanism and the compact object environment from electromagnetic signals. Fortuitously, CCSNe produce two extra messengers: neutrinos and gravitational waves (GWs); both carry information from the stellar core to the observer with negligible interference along the way (*4–6*). Numerical studies (*7, 8*) showed that CCSNe can be highly asymmetric, giving rise to a substantial time-dependent gravitational quadrupole moment, which generates GW emission. However, with a small fraction $(E \approx 10^{46}\ \mathrm{erg})$ of the CCSN energy going in GW production, the Advanced Laser Interferometer GW Observatory (LIGO) (*9*) can detect only nearby ($\lesssim 1$ Mpc) events (*10*).

$E_\nu \sim 3\ 10^{53}$ erg

Intro: the case of collapsars associated to LGRBs
Jet: GW emission at low frequency (<Hz)

A special class of CCSNe - collapsars (*11*) is associated with long-duration gamma-ray bursts (LGRBs), which originate in energetic jets powered by a rapidly rotating newly-formed compact object, a black-hole (BH) or a neutron star. Their enormous power makes LGRB jets promising GW sources. The GW memory effect (*12, 13*) implies that the GW frequency is inversely proportional to the timescale over which the metric is perturbed. For jets, this timescale is set by the longer of the launching and acceleration timescales (*14–20*). Thus, the characteristic duration of LGRBs $\gtrsim 10$ s places the GW emission from LGRB jets at the sub-Hz frequency band, too low for LIGO, but potentially detectable by the proposed space-based Decihertz Interferometer GW Observatory (*21*).

$$f \simeq \frac{1}{t_{\rm perturb}}$$

$$t_{\rm perturb} = \max\left(t_{\rm launch}; t_{\rm acc}\right)$$

$$t_{\rm perturb} > 1\,{\rm s}$$

$$f < 1\,{\rm Hz}$$

LGRB: cocoon

As the jets drill their way out of the collapsing star, they shock the dense stellar material and build a cocoon - a hot and turbulent structure that envelops the jets (Fig. 1) (*22–24*). The cocoon is generated as long as parts of the jets are moving sub-relativistically inside the star. LGRB jets break out from the star after $t_b \approx 10$ s (*25*) and spend a comparable amount of time outside of the star before their engine turns off (*26*). After breakout, jets are expected to stop depositing energy into the cocoon (*22, 27*), unless they are intermittent or wobbly (*28, 29*). This implies that the cocoon energy $E_c \approx 10^{51} - 10^{52}$ erg (*30*) is at least comparable to that of the jet (the energy retained by the jet after breakout), $E_c \gtrsim E_j$.

Cocoon: sub-mildly relativistic

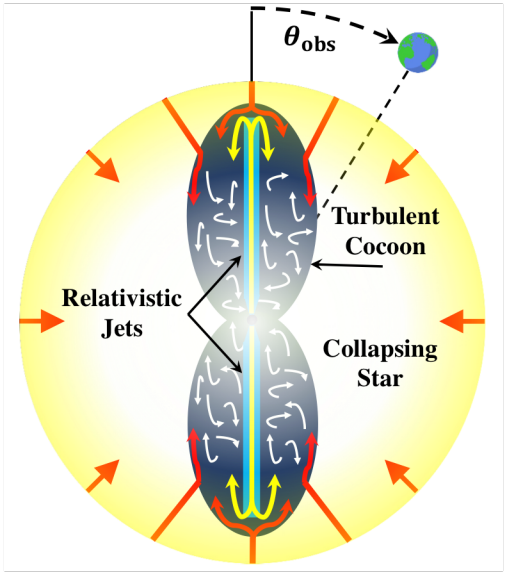

Figure 1: Jets (light blue) inflate the energetic cocoon (dark blue) inside of a dying massive star (pale yellow). The jets run into and shock against the collapsing star, forming a backflow (yellow arrows). Infalling star runs into and shocks against the backflow (red arrows). The shocked jet and shocked stellar components form the cocoon and turbulently mix inside of it (white arrows).

LGRB: GW emission from the cocoon - strain

Here, we argue that the cocoon is an attractive new GW source in present-day detectors. First, the cocoon evolves over shorter timescales than the jets, and, as we show below, its GW signal lies within LIGO frequency band. Second, relativistic jets are subject to the anti-beaming effect (*31*) that inhibits the GW emission within their opening angle, whereas the cocoon can emit GWs in all directions across the sky.

The GW strain can be approximated as

$$h \approx \frac{2G}{Dc^4}\frac{d^2Q}{dt^2}\,, \tag{1}$$

where G is the gravitational constant, c is the speed of light, D is the distance to the source, and Q is the gravitational quadrupole. From Eq. 1, cocoon-powered GW characteristic strain is (*10*)

$$h_{\rm coc} \approx \frac{4G}{Dc^4}E_c\epsilon \approx 10^{-23}\,\frac{100\ {\rm Mpc}}{D}\frac{E_c\epsilon}{10^{52}\ {\rm erg}}\,, \tag{2}$$

where ϵ is the degree of asymmetry of the cocoon, which depends on the viewing angle $\theta_{\rm obs}$ (see Fig. 1).

$$\frac{{\rm d}^2Q}{{\rm d}t^2} \sim \frac{Q}{t^2} \sim \frac{\epsilon MR^2}{(R/\beta c)^2} \sim \epsilon\beta^2 Mc^2 \quad ?$$

3D GRMHD simulations

We carry out a high resolution 3D general-relativistic magnetohydrodynamic (GRMHD) simulation of energetic LGRB jets in a collapsing star by repeating the simulation from (*29*), but with an increased data output frequency, as needed to resolve the time-variability of the gravitational quadrupole. This simulation follows the jets from the BH for ≈ 3.1 s until they reach distance $\approx 1.5R_\star$ and energy $E_j \approx 2.5 \times 10^{52}$ erg, where $R_\star$ is the stellar radius. Fig. 2 depicts the hourglass-shaped cocoon upon breakout from the star (see the full animation and accompanying sonification in `https://oregottlieb.com/gw.html`). For observers facing the jet axis (Fig. 2a), the projected shape of the cocoon is close to circular ($\epsilon \ll 1$), significantly suppressing the quadrupole moment. Off-axis observers (Fig. 2b,c), on the other hand, will see an asymmetric cocoon with an order unity asymmetry $\epsilon \approx 1$, thus maximizing the observed GW signal strain amplitude in Eq. 2.

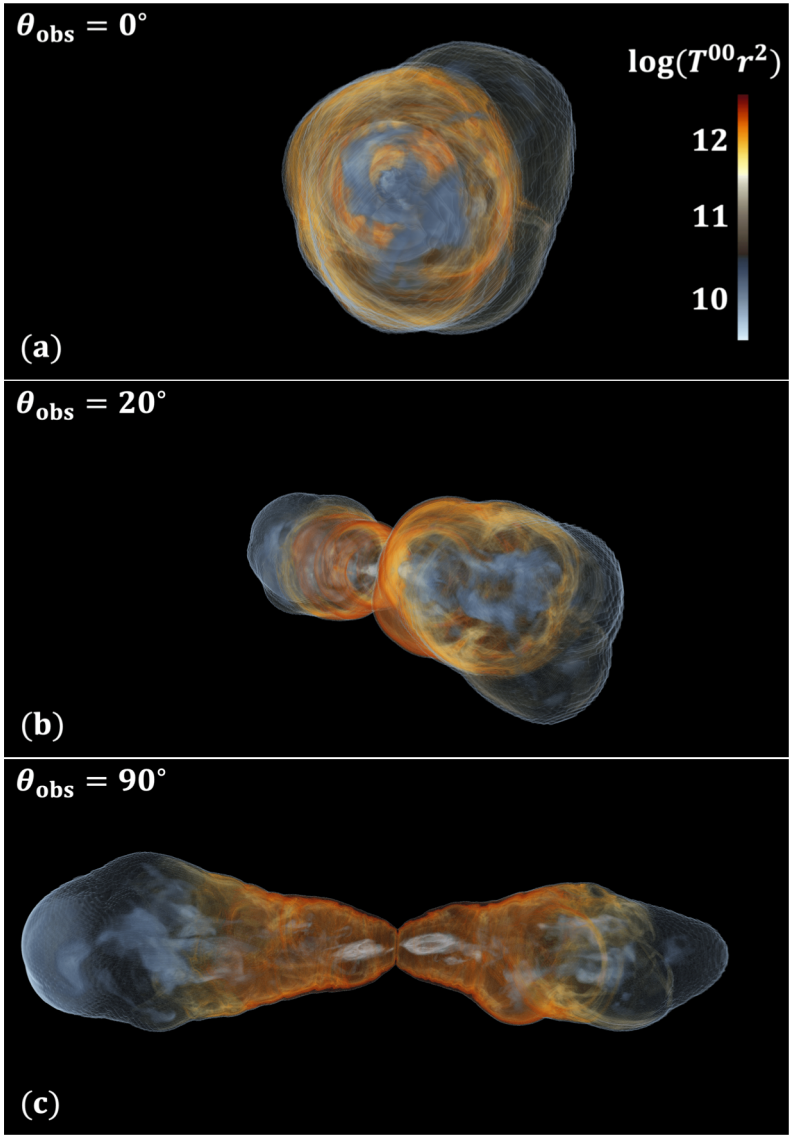

Figure 2: Three-dimensional (3D) rendering of the cocoon upon breakout from the star at different viewing angles. At $\theta_{\rm obs} = 0°$ (a) the axisymmetric projection results in a weak on-axis signal as the cocoon appears nearly circular, whereas at larger angles the asymmetric shape of the cocoon enables strong GW emission (b,c). The colormap delineates $\log(T^{00}r^2)$ in c.g.s., which is an order of magnitude estimate to the gravitational quadrupole density, where T^{00} is the contravariant energy density component of the stress-energy tensor. See details in supplementary materials in (*32*).

3D GRMHD simulations: GW signal (1) estimate of the frequency range

Turbulent motions in the jet[1]-cocoon result in a stochastic GW signal, and lead to a broad spectrum of GW frequencies that is challenging to evaluate analytically. However, we can estimate the main features of the emerging GW spectrum frequency range as follows. The smallest length-scales of the cocoon emerge over the thickness of the shocked region $\Delta r_{\rm sh} \approx 10^{-2} R_\star \Gamma^{-2} \approx 10^8$ cm (*33*), where $\Gamma \approx 3$ is the jet head Lorentz factor inside the star, and $R_\star \approx 10^{11}$ cm. These shocked regions evolve over $t_{\rm min} \approx \Delta r_{\rm sh}/c_s \approx 2 \times 10^{-3}$ s, where $c_s \approx c/\sqrt{3}$ is the relativistic sound speed, implying the highest GW frequency, $f_{\rm max} \approx t_{\rm min}^{-1} \approx 0.5$ kHz. The maximum timescale is the time that the jet energizes the cocoon, $t_{\rm max} \gtrsim t_b \approx 10$ s, thereby setting the minimum GW frequency, $f_{\rm min} \approx t_{\rm max}^{-1} \lesssim 0.1$ Hz. The cocoon energy is distributed quasi-uniformly in the logarithm of the proper-velocity, $10^{-2.5} \lesssim \Gamma\beta \lesssim 3$ (*27, 29*). Thus, although various cocoon components evolve on different timescales, they carry comparable amounts of energy, and are expected to result in a flat GW spectrum between $f_{\rm min}$ and $f_{\rm max}$.

[1]Jets are also subject to instabilities (*28, 29*) that may introduce high frequency GWs. Computing those requires going beyond analytic and numerical modeling that assume continuous and steady axisymmetric jets.

$R_\star = 10^{11}\,\mathrm{cm}$

$\Gamma = 3$

$$t_{\rm min} \simeq \frac{\Delta R_{\rm sh}}{c_{\rm S}} \simeq \sqrt{3}\,10^{-2}\,\frac{R_\star}{\Gamma^2 c} \simeq 2\,10^{-3}\,\mathrm{s}$$

$$t_{\rm max} \simeq t_{\rm b} \simeq 10\,\mathrm{s}$$

3D GRMHD simulations: GW signal (2) numerical

To compute the GW signal, we post-process $\gtrsim$ petabyte of simulation data output at a high cadence, enabling us to numerically calculate the second derivatives of the gravitational quadrupole moment (see Supplementary Materials in (*32*))[2]. Fig. 3a,b shows a 3D mass density rendering of the cocoon after breakout from the star, taken from (*29*). Similar to its pre-breakout shape in Fig. 2, the cocoon is asymmetric when observed off-axis (Fig. 3a), and near-axisymmetric when observed on-axis (Fig. 3b). In fact, the strain amplitudes in Fig. 3c,d show that on-axis emission is weaker by 1-2 orders of magnitude than off-axis emission, whose spectrum is roughly flat at $0.1\ \mathrm{kHz} \lesssim f \lesssim 0.6\ \mathrm{kHz}$, followed by an exponential cutoff, $h(f) \propto \exp\left[-(f/0.6\ \mathrm{kHz})^2\right]$ (dotted line), consistent with our $f_{\rm max}$ estimate. The off-axis strain amplitude spectrogram (Fig. 3e) shows that as the cocoon expands ($t \lesssim 1.2$ s in our simulation), the GW emission turns on, intensifies and shifts only slightly toward lower frequencies, as the spectrum does not vary considerably between different regions in the cocoon, owing to mixing. At ≈ 1.2 s, the jets traverse about third of the star, the cocoon is fully formed, and the signal plateaus. The GW emission is expected to last until the jet engine shuts off at t_j (longer than our simulation), and the cocoon turbulent motions relax[3]. On the other hand, the on-axis GW signal becomes gradually stronger as the jet breaks out from the star (Fig. 3f), owing to a stronger deviation from axisymmetry in the absence of a cocoon confinement by the dense stellar envelope after breakout. Both on- and off-axis signals are qualitatively different from traditional GWs in CCSNe whose peak frequency rises over a much shorter GW emission timescale ($\ll 1$ s) (*34, 35*).

[2]For comparison, in (*32*) we also calculate the weak GW signal from non-jetted explosions, whose emission is dominated by an expanding accretion shock.

3D GRMHD simulations: GW signal (2) numerical

Strong signal reduction for on-axis observer.

Simulation ends before the central engine shuts off

Detectability in LV data?

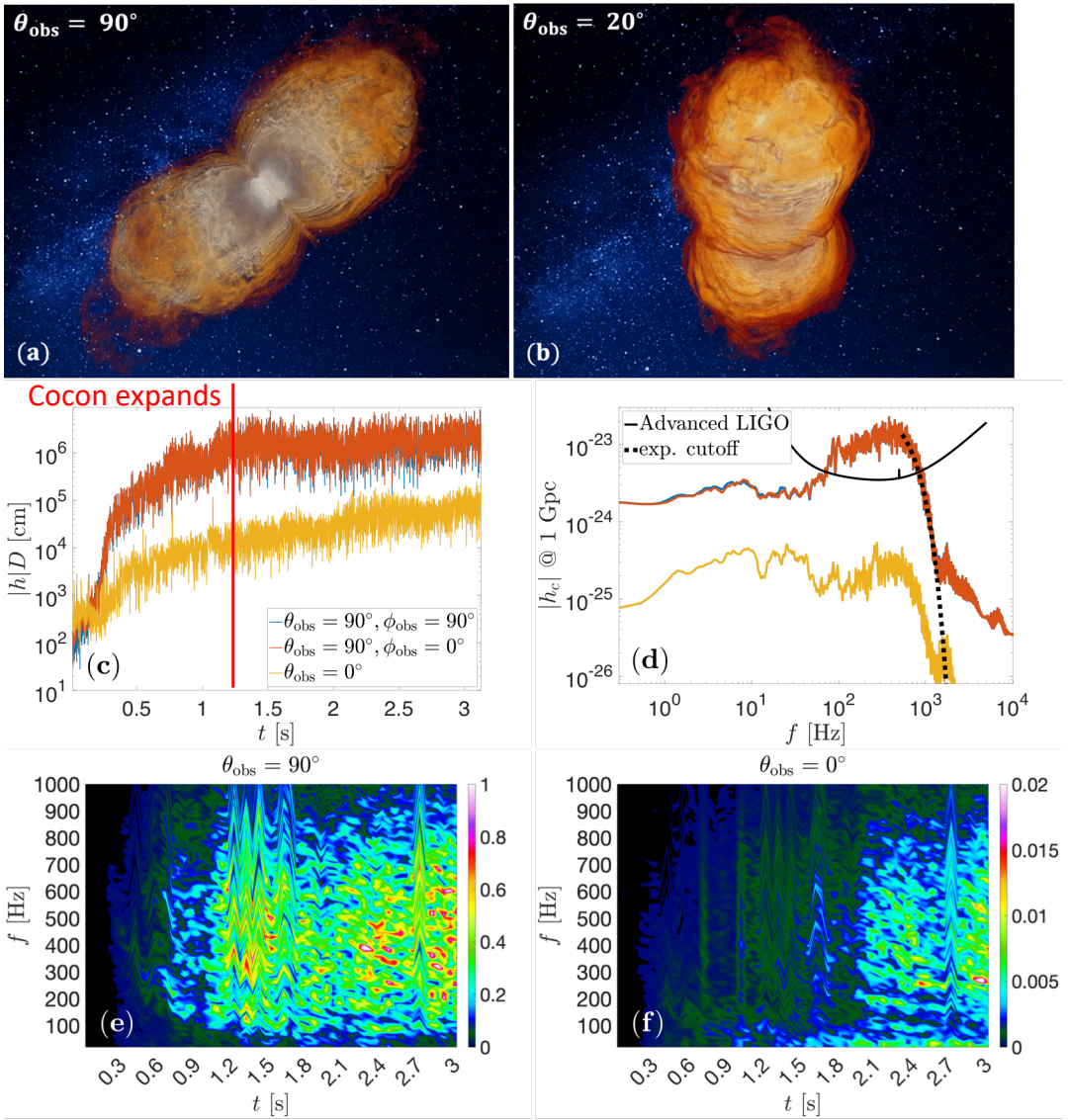

Figure 3: 3D rendering of off-axis (a) and on-axis (b) projections of the cocoon mass density after breakout from the star (star is in the center shown in white), taken from (*29*). On- and off-axis strain amplitude in time (c) and frequency (d) domains. Normalized amplitude (by maximal off-axis amplitude) spectrograms for a sliding window of 50 ms for (average of $\phi_{obs} = 0°$ and $\phi_{obs} = 90°$) off-axis (e) and on-axis (f) observers. The off-axis amplitude is constant in frequency at 0.1 kHz $\lesssim f \lesssim 0.6$kHz, and in time from ≈ 1 s until the jet shuts off and the cocoon relaxes.

Estimated rates? (1) scaling for the strain

The off-axis GW emission from the energetic cocoon ($E_c \approx 2E_j \approx 5 \times 10^{52}$ erg) is detectable out to distances as far as ≈ 1 Gpc (Fig. 3d), in agreement with Eq. 2 (to within a factor of two). For on-axis observers the GW detection horizon of such cocoons is much smaller ≈ 20 Mpc, owing to the low degree of non-axisymmetry which renders a direct on-axis detection unlikely. We use our numerical result to calibrate Eq. 2, assuming a linear scaling of the strain amplitude with the cocoon energy[4],

$$h_{\rm coc} = 10^{-23}\,\frac{200\,{\rm Mpc}}{D}\,\frac{E_c\epsilon}{10^{52}\,{\rm erg}}\,. \tag{3}$$

Approximating $E_c \approx E_j$ and $\epsilon(\theta_{\rm obs}) \approx 1$, we can express Eq. 3 via the BH spin a, mass $M_{\rm BH}$ and magnetic field strength on the horizon $B_{\rm BH}$, assuming that the jet is powered by the Blandford-Znajek mechanism (*36–38*),

$$h_{\rm coc} \gtrsim 10^{-23}\,\frac{200\,{\rm Mpc}}{D}\left(\frac{t_j}{10\,{\rm s}}\right)\left(\frac{M_{\rm BH}}{5\,{\rm M}_\odot}\frac{B_{\rm BH}}{10^{15}\,{\rm G}}\frac{a}{0.8}\right)^2\,. \tag{4}$$

Therefore, detections of cocoon-powered GWs can help us constrain the properties of the central BH and its environment deep inside the dying star.

$E_{\rm c} \simeq E_{\rm j} \simeq E_{\rm BZ}$

Estimated rates? (2) LGRB-collapsar rate

To estimate the expected number of detectable GW events in LIGO observing run O4, we connect E_c to the observed jet energy via $E_c \approx E_j = \xi E_{j,\rm obs}$, and consider two types of jets with

[3]GW travel time effects may slightly prolong the signal duration for observers close to the jet axis, see (*32*).

[4]We neglect secondary effects on the cocoon-powered GW emission, such as the density profile of the star and turbulent mixing, that may affect the cocoon shape and its GW spectrum, and cause deviations from the linear scaling shown in Eq. 2.

Wobbling jet scenario ?

opening angle $\theta_j \approx 0.1^{+0.07}_{-0.03}$ rad (*39*): i) a traditional axisymmetric jet, for which we adopt $\xi = 1$ and conventional local LGRB rate $\mathcal{R}_{\rm GRB} \approx 100\ {\rm Gpc^{-3}\ yr^{-1}}$ (*40*); and ii) a jet wobbling by $\theta_w \approx 0.2$ rad as in our simulations, for which the local GRB rate is an order of magnitude lower (*29*). When a jet wobbles by $\theta_w \approx 2\theta_j$, it is observed on average only $(\theta_j/\left[\theta_w + \theta_j\right])^2 \approx 10\%$ of the time, namely $\xi = 10$. Assuming the γ-ray energy is half of the total jet energy (*41*), the isotropic equivalent γ-ray energy is $E_{\gamma,\rm iso} \approx \theta_j^{-2} E_{j,\rm obs}$. The distribution of LGRBs in $E_{\gamma,\rm iso}$ can be approximated by a power-law (*42*), which we find to be $N_{\rm LGRBs} \propto {E_{\gamma,\rm iso}}^{-1.5}$. This implies that the most energetic GRBs dominate cocoon-powered GW detections, so that the $E_{\gamma,\rm iso}$ power-law cutoff, $E_{\gamma,\rm iso,m}$ sets the expected number of detectable events, see (*32*).

Needs to assume beaming angle, local rate, luminosity function.
Here standard values but highly uncertain.

Estimated rates? (3) Results for O4

Assuming the LIGO detection threshold of the characteristic strain at the relevant frequencies, $|h_{\rm crit}| \approx 10^{-23}$ and isotropic GW emission ($\epsilon\,(\theta_{\rm obs}) \approx 1$), we use Eq. 3 to show in Fig. 4 the number of detectable cocoon-powered GW events per year in the upcoming LIGO observing run O4 for the above two types of jets (*32*), where the shaded areas depict the standard deviation in θ_j. If jets propagate along a fixed axis, the detection probability (red line) is $\gtrsim 10\%$. If jets wobble (blue line), then a jet (and the jet-powered cocoon) has more energy for a given $E_{\gamma,\rm iso}$, since most of its energy ($\approx 90\%$) is beamed away from our line of sight. This dramatically increases the expected number of detectable GW events to ≈ 10 during observing run O4. Had the latter case been the true rate, then such events were likely detectable in previous LIGO runs. However, this signal was never explicitly searched for, and might be easily overlooked due to its noisy nature compared to inspiral GWs. This raises the exciting possibility that existing LIGO data already contains cocoon-powered GW signals. We emphasize that the large uncertainties in θ_j, the distribution of the most energetic GRBs, and the prompt/afterglow energy ratio, in turn introduce large uncertainties in the expected number of detectable GW events[5]. Interestingly,

[5] Additionally, in our estimate we ignore jets that are choked in the stellar envelope and do not generate a GRB. If such phenomenon is common among massive stars (*38*), then the predicted cocoon-powered GW detection rate is increased significantly, see (*32*).

the detection rate of quasi-isotropic GWs from cocoons with energies $E_c < E_{\rm max}$ constrains the fraction of SN Ib/c progenitors that power LGRBs with $E_c < E_{\rm max}$, as shown on the right vertical axis in Fig. 4, see (*32*).

Wobbling jet scenario: higher rates, already in pre-O4 data?

Estimated rates? (3) Results for O4

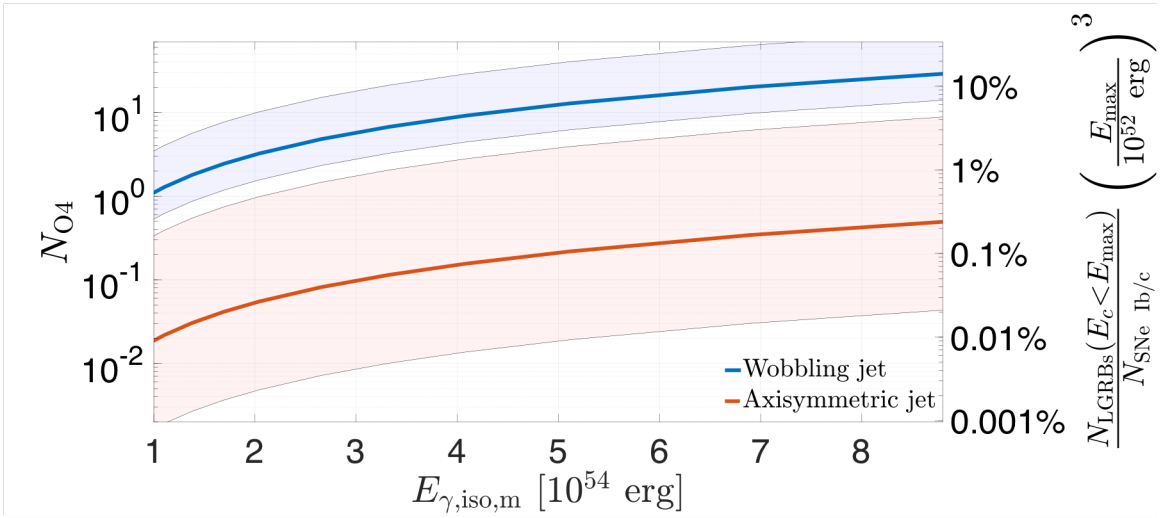

Figure 4: The number of detectable cocoon-powered GW events in one year of LIGO observing run O4 as a function of the maximal isotropic equivalent γ-ray energy $E_{\gamma,\rm iso,m}$ (the cutoff of the power-law fit to $N_{\rm LGRBs}(E_{\gamma,\rm iso})$ distribution), assuming LIGO detection threshold of $|h_{\rm crit}| = 10^{-23}$ and isotropic GW emission. If the jets propagate along a fixed axis, then $\gtrsim 0.1$ events are expected (red line), whereas if jets wobble (blue line), multiple GW events are likely to be detectable. Variations in jet opening angle (shaded areas) introduce uncertainties into predicted GW detection rate. The detection rate of cocoons with $E_c < E_{\rm max}$ also indicates the abundance of LGRBs with such cocoons among SNe Ib/c (right vertical axis labels).

Associated em emission?

LGRB: not favored (GW strongly reduced for on-axis observer) - SN+cocoon
- shock breakout (s-min) = difficult
- SN+cooling cocoon (days-months)
- afterglow (days-years)

LGRBs are likely to be rich multi-messenger events. While a coincident LGRB-GW detection is unlikely due to the weak on-axis GW emission, the GW signal is likely accompanied by a wide range of electromagnetic counterparts powered by the SN explosion and the cocoon: shock breakout in γ- and X-rays (seconds to minutes), cooling emission and radioactive decay in UV/optical/IR (days to months), and broadband synchrotron (afterglow) emission (days to years) (*30, 43*). The earliest radiative signal emerges when the cocoon or SN shock wave breaks out from the star, producing a nearly coincident electromagnetic counterpart to the cocoon-powered GWs. However, the shock breakout signal originates in a thin layer, and primarily depends on the breakout shell velocity and structure of the progenitor star, rather than the total explosion energy (*33, 44*). Thus, whereas under favorable conditions of viewing angle and progenitor structure it is possible to detect a shock breakout in γ-rays, those signals will typically go unnoticed.

Shock breakout

Associated em emission?

LGRB: not favored (GW strongly reduced for on-axis observer) - SN+cocoon
- shock breakout (s-min) = difficult
- SN+cooling cocoon (days-months)
- afterglow (days-years)

After releasing the shock breakout emission, the stellar shells and the cocoon expand adiabatically and give rise to an optical cooling signal. SNe Ib/c cooling emission lasts weeks and peaks at an absolute magnitude $M_{\rm AB} \approx -18$ (*45*), whereas cocoons with energies of $E_c \gtrsim 10^{52}$ erg that emit strong GWs, will power even brighter ($M_{\rm AB} \lesssim -19$) quasi-isotropic ($\theta_{\rm obs} \lesssim 1.0$ rad) UV/optical cooling emission on timescales of days (*30, 46*). The cocoon cooling emission is sufficiently long and bright to be detected at most relevant distances of $\lesssim 1$ Gpc by Zwicky Transient Facility (ZTF) (*47, 48*) and upcoming Rubin Observatory (*49*), with most of these signals will be accompanied by the detection of the longer SN emission. Furthermore, cocoons with $E_c \gtrsim 10^{52}$ erg s^{-1} will explode the entire massive star and may power superluminous supernovae (SLSNe) with $M_{\rm AB} \lesssim -21$ (*50*) over $\approx$ months timescale.

SN+cooling cocoon

Associated em emission?

LGRB: not favored (GW strongly reduced for on-axis observer) - SN+cocoon

- shock breakout (s-min) = difficult
- **SN + cooling cocoon (days-months)**
- **afterglow (days-years)**

Finally, the interaction of such energetic cocoons with the circumstellar medium will produce a detectable broadband afterglow, assuming typical ambient densities and standard equipartition parameters (*51*). The timescale over which the afterglow emission emerges varies from days to years, as it depends on the specific parameters of the system and the observer's viewing angle, thereby posing a challenge to its detection. However, the early cooling signal that can be detected by a rapid search will enable an early localization of the event and a targeted search for the later multi-band afterglow, which will potentially alleviate the afterglow detection difficulty.

Afterglow:
easier if SN+cocoon
already detected

ZTF+LVK runs: targeted searches

In fact, the ZTF online catalog (*52*) already contains ≈ 100 CCSNe Ib/c/SLSNe that were detected during LIGO observing run O3. 14 of these are SNe Ic-BL: the only confirmed SN type to be associated with LGRBs (*53*). About 50 of these CCSNe (and 10 SNe Ic-BL) lie within 170 Mpc of Earth, implying that if their progenitors harbored (off-axis) GRBs with conventional $E_c \lesssim 10^{52}$ erg (*30*), GWs from their cocoon should be detectable in LIGO data. We will perform a targeted search for GWs from these progenitors in a follow-up work.

Conclusion

In this report, we propose and investigate the first non-inspiral GW source that is detectable by LIGO out to hundreds of Mpc. Future calculations of the zoo of cocoon-powered GWs for different LGRB progenitors will enable the production of detailed templates of these signals, and will be addressed in a follow-up work. This will enable a more efficient search for GWs from collapsar cocoons, enhance the wealth of information regarding the physical properties of the source to be extracted from the GW signal, and aid follow-up searches for electromagnetic counterparts of these multi-messenger events, ultimately providing a better understanding of the relation between CCSNe and LGRBs.

GW templates?